U.S. DEPARTMENT OF ENERGY
National Nuclear Security Administration
SAND2011-4879C

Office of Nonproliferation and Verification Research & Development

Improved Growth of CZT Crystals

Independent Review Meeting

Xiaowang Zhou

Sandia National Laboratories

July 27, 2011

Project Team

F. P. Doty (PI), SNL/CA
X. W. Zhou, D. K. Ward, B. M. Wong, SNL/CA
Qiming Li, SNL/NM

Sandia National Laboratories

Ideal Atomistic Model for Defects

1. **Transferrable to a variety of configurations: clusters** (dimer, trimer, square, tetrahedron, and chain for elements and compounds; Cd_2Te and $CdTe_2$ trimers for compounds)**, lattices** (diamond-cubic, simple-cubic, body-centered-cubic, face-centered-cubic, hexagonal-close-packed, graphite, graphene, and A8 for elements; zinc-blende, wurtzite, NaCl, CsCl, binary-graphite, AuCu, CuPt, NiAs, CrB, AlSb, binary-graphene, and face-centered-square for the stoichiometric compound CdTe; Ag_2O, CaF_2 for the non-stoichiometric compounds $CdTe_2$ or Cd_2Te)**, and defects** (vacancies, Cd@Te and Te@Cd antisites, Cd and Te interstitials at different locations)**;**
2. **Lowest energy for the equilibrium structure;**
3. **Validatable in vapor- and melt- growth simulations: testing a variety of configurations that are not possible to study directly.**

Current Status in the Field

1. Stillinger-Weber (SW) potentials are most widely used (~2300 citations);
2. Tersoff/Brenner potentials are second-widely used (~1300 citations);
3. Simulations of crystalline growth are limited to vapor deposition; convincing cases for melt-growth are yet to be demonstrated;
4. Most successful simulations of crystalline growth of vapor deposition were achieved using SW potentials;
5. Many Tersoff literature potentials were found to predict amorphous growth in vapor deposition simulations.

Stillinger-Weber (SW) Potential

$$E = \frac{1}{2}\sum_{i}\sum_{j\neq i}\left[R_{ij}\left(r_{ij}\right)-U_{ij}\left(r_{ij}\right)\right]+\frac{1}{2}\sum_{i}\sum_{j\neq i}\sum_{k\neq j\neq i}u_{ij}\left(r_{ij}\right)\cdot u_{ik}\left(r_{ik}\right)\cdot\left[\cos\left(\theta_{jik}\right)+\frac{1}{3}\right]^{2}$$

$$\phi_{ij}\left(r_{ij}\right)=R_{ij}\left(r_{ij}\right)-U_{ij}\left(r_{ij}\right)=\begin{cases}\varepsilon_{ij}A_{ij}\left(\dfrac{B_{ij}}{r_{ij}^{4}}-1\right)\exp\left(\dfrac{\sigma_{ij}}{r_{ij}-a_{ij}\sigma_{ij}}\right) & , \quad r_{ij}\leq a_{ij}\sigma_{ij} \\ 0 & , \quad r_{ij}>a_{ij}\sigma_{ij}\end{cases}$$

$$u_{ij}\left(r_{ij}\right)=\begin{cases}\sqrt{\varepsilon_{ij}\lambda_{ij}}\exp\left(\dfrac{\gamma_{ij}\sigma_{ij}}{r_{ij}-a_{ij}\sigma_{ij}}\right) & , \quad r_{ij}\leq a_{ij}\sigma_{ij} \\ 0 & , \quad r_{ij}>a_{ij}\sigma_{ij}\end{cases}$$

ε_{ij}, λ_{ij},, γ_{ij}, A_{ij}, B_{ij}, σ_{ij}, a_{ij}, are parameters, and $\sigma_{ij}\cdot a_{ij}$ is cutoff distance.

F. H. Stillinger, and T. A. Weber, Phys. Rev. B, 31, 5262 (1985).

Stillinger-Weber Potential Observations

$$E = \frac{1}{2}\sum_{i}\sum_{j\neq i}\left[R_{ij}\left(r_{ij}\right)-U_{ij}\left(r_{ij}\right)\right]+\frac{1}{2}\sum_{i}\sum_{j\neq i}\sum_{k\neq j\neq i}u_{ij}\left(r_{ij}\right)\cdot u_{ik}\left(r_{ik}\right)\cdot\left[\cos\left(\theta_{jik}\right)+\frac{1}{3}\right]^{2}$$

1. The angular term is essentially a parabolic energy penalty for deviation of bond angle from the tetrahedral angle.
2. The angular term modifies a repulsive interaction. From quantum mechanics theories, the repulsive interaction is well approximated by a pair interaction, and it is the attractive interaction that depends more on electron orbital and bond angles.
3. Any non-tetrahedral structures would have longer bond lengths than that of the tetrahedral structures.
4. SW potentials work well for tetrahedral structures, but are not transferrable to defects and other metastable phases.

Relative Hardness

In pair potential model, the system energy E is expressed as

$$E = \frac{1}{2}\sum_{i=1}^{N}\sum_{\substack{j=1 \\ j\neq i}}^{N}\left[R_{ij}\left(r_{ij}\right) - U_{ij}\left(r_{ij}\right)\right]$$

Where R(r) and U(r) represent repulsive and attractive interactions. The relative hardness is defined as

$$H = \frac{R'_{ij}\left(r_{e,ij}\right)/R_{ij}\left(r_{e,ij}\right)}{U'_{ij}\left(r_{e,ij}\right)/U_{ij}\left(r_{e,ij}\right)} \sim 2$$

The potential behaves well when H approximately equals 2 (otherwise double energy minimums might occur when the system is hydrostatically strained).

Stillinger-Weber Potential Parameterization

$$E = \frac{1}{2}\sum_{i}\sum_{j\neq i}\left[R_{ij}\left(r_{ij}\right)-U_{ij}\left(r_{ij}\right)\right]+\frac{1}{2}\sum_{i}\sum_{j\neq i}\sum_{k\neq j\neq i}u_{ij}\left(r_{ij}\right)\cdot u_{ik}\left(r_{ik}\right)\cdot\left[\cos\left(\theta_{jik}\right)+\frac{1}{3}\right]^{2}$$

1. When a ground state tetrahedral structure (dc or zb) is subject to a hydrostatic strain, the SW potential reduces to a pair potential.
2. The four parameters of the pair part of the SW potential can be completely determined from four properties of the ground state phase: lattice constant, cohesive energy, bulk modulus, and relative hardness.
3. As long as the angular prefactor λ is above a critical value, the ground state tetrahedral structure is guaranteed to have the lowest energy. Only when this is satisfied, other shear moduli of the ground state structure can be fitted. Most literature do not even bother to fit angular parameters: they just use $\lambda = 32.5$ and $\gamma = 1.2$!

1. F. H. Stillinger, and T. A. Weber, Phys. Rev. B, 31, 5262 (1985).
2. A. Béré and A. Serra, Phys. Rev. B, 65, 205323 (2002).

SW Potential Growth Simulations

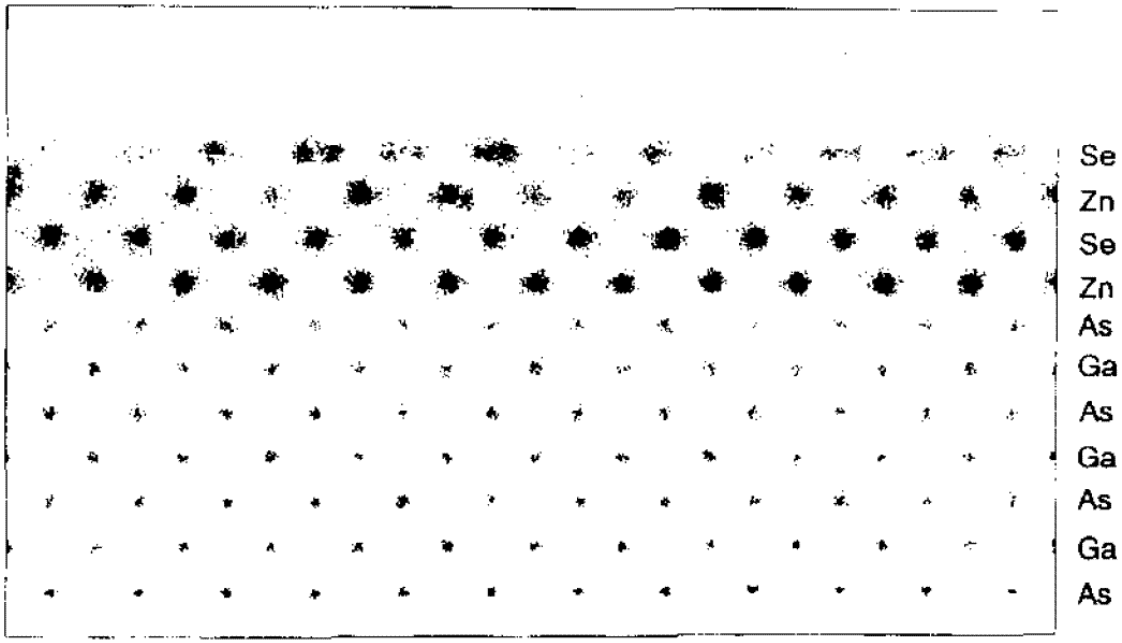

Growth of ZnSe on As-terminated (001) GaAs surface. – from Ref. [1].

1. G. H. Grein, J. P. Faurie, V. Bousquet, E. Tournie, R. Benedek, and T. de la Rubia, J. Cryst. Growth, 178, 258(1997).
2. G. H. Gilmer, and C. Roland, Appl. Phys. Lett., 65, 824(1994).
3. B. Strickland, and C. Roland, Phys. Rev. B, 51, 5061(1995).
4. H. W. Lu, and J. Y. Feng, Modelling Simul. Mater. Sci. Eng., 8, 621(2000).

SW Potentials "Easily" Simulate Crystalline Growth

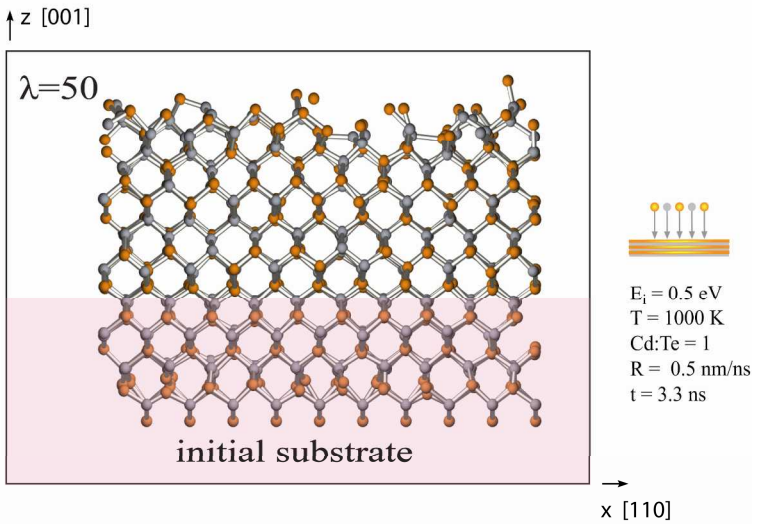

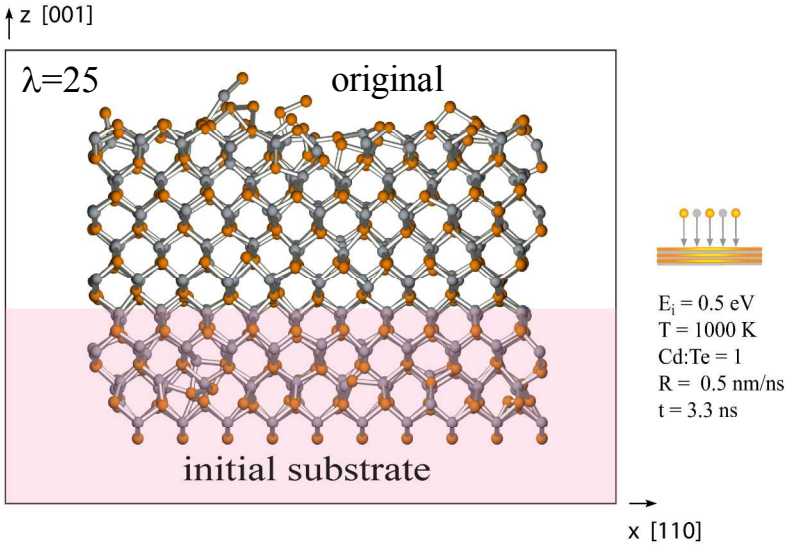

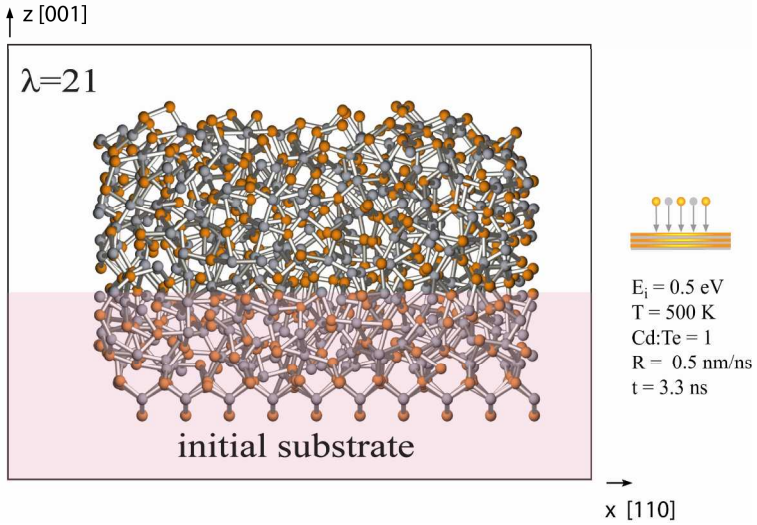

CdTe potential from Z. Q. Wang, D. Stroud, and A. J. Markworth, Phys. Rev. B, 40, 3129 (1989).

Tersoff Potential

$$E = \frac{1}{2}\sum_i \sum_{j \neq i} \left[\phi_{ij}(r_{ij}) - \psi_{ij}(r_{ij}) \cdot B_{ij} \right]$$

$$B_{ij} = \chi_{ij} \cdot \left(1 + \beta_{ij}^{n_{ij}} \cdot \zeta_{ij}^{n_{ij}}\right)^{-\frac{1}{2n_{ij}}}$$

$$\zeta_{ij} = \sum_{\substack{k=1 \\ k \neq i,j}}^{N} f_{ik}(r_{ik}) \cdot \omega_{ik} \cdot g_{ik}(\theta_{jik})$$

$$g_{ij}(\theta) = \gamma_{ij}\left[1 + \frac{c_{ij}^2}{d_{ij}^2} - \frac{c_{ij}^2}{d_{ij}^2 + (h_{ij} + \cos\theta)^2}\right]$$

$$\varphi_{ij}(r_{ij}) = f_{ij}(r_{ij}) \cdot V_{R,ij}(r_{ij})$$

$$\psi_{ij}(r_{ij}) = f_{ij}(r_{ij}) \cdot V_{A,ij}(r_{ij})$$

$$f_{ij}(r_{ij}) = \begin{cases} 1, & r_{ij} \leq r_{1,ij} \\ \frac{1}{2} + \frac{1}{2}\cos\left[\frac{\pi(r_{ij} - r_{1,ij})}{r_{c,ij} - r_{1,ij}}\right], & r_{1,ij} < r_{ij} < r_{c,ij} \\ 0, & r_{ij} \geq r_{c,ij} \end{cases}$$

$$V_{R,ij}(r_{ij}) = A_{ij} \cdot \exp(-\lambda_{ij} \cdot r_{ij})$$

$$V_{A,ij}(r_{ij}) = B_{ij} \cdot \exp(-\mu_{ij} \cdot r_{ij})$$

A_{ij}, B_{ij}, λ_{ij}, μ_{ij},, χ_{ij}, β_{ij}, n_{ij}, ω_{ij}, γ_{ij}, c_{ij}, d_{ij}, h_{ij}, $r_{1,ij}$, and $r_{c,ij}$ are parameters.

J. Tersoff, Phys. Rev. B, 39, 5566 (1989).

Tersoff Potential Observations

$$E = \frac{1}{2}\sum_{i}\sum_{j\neq i}\left[\phi_{ij}\left(r_{ij}\right) - \psi_{ij}\left(r_{ij}\right)\cdot B_{ij}\right]$$

1. The angular term modifies an attractive interaction. It is consistent with the concepts of quantum mechanics theories that the repulsive interaction is well approximated by a pair interaction, and it is the attractive interaction that depends more on electron orbital and bond angles.
2. In particular, Tersoff potential can be viewed as a simple bond order potential that can be derived directly from quantum mechanics theories. Here B_{ij} can be viewed as bond order which is defined as half of the difference of the number of electrons in the bonding and the anti-bonding states, and $\psi_{ij}(r_{ij})$ is the bond integral which describes the probability for electrons to hop from one orbital to another.
3. Tersoff potential is fundamentally more transferrable than SW potential, but there is no obvious approach to stabilize the tetrahedral structure. Explicit considerations of a variety of phases and defects are mandatory!

Failed Tersoff Potential Growth Simulations

InAs on (110) GaAs[1].

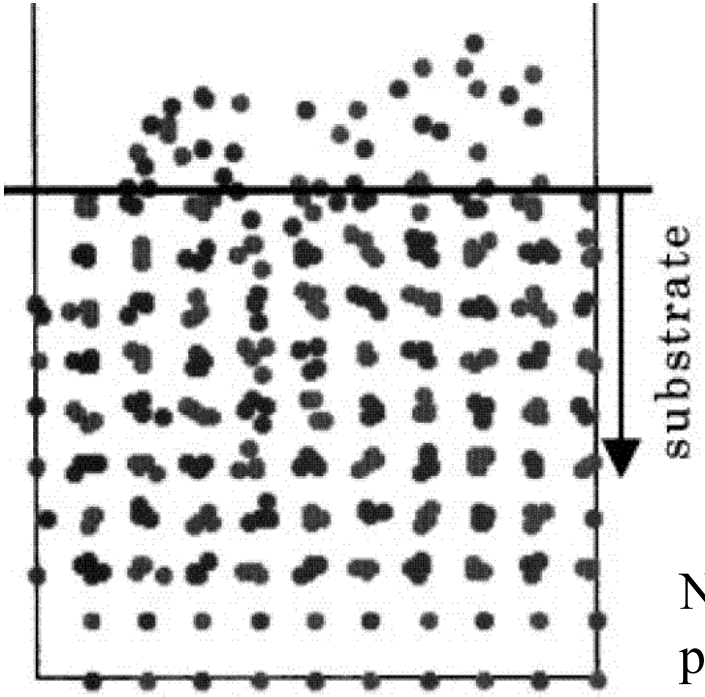

(100) CdTe[5,6].

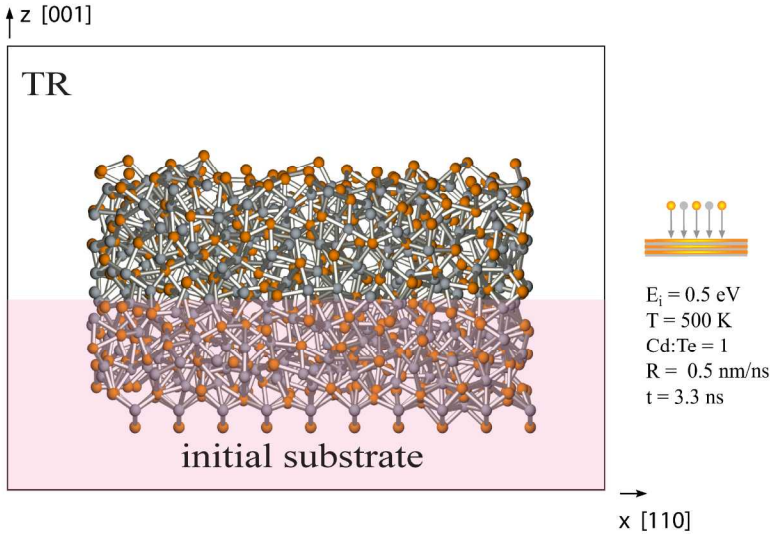

None of the potentials listed here correctly predicts the crystalline growth.

1. M. Nakamura, H. Fujioka, K. Ono, M. Takeuchi, T. Mitsui, and M. Oshima, J. Cryst. Growth, 209, 232(2000).
2. J. Tersoff, Phys. Rev. B, 39, 5566(1989). – for Si (amorphous growth, but can re-crystallize at 2200 K through bulk transformation).
3. P. A. Ashu, J. H. Jefferson, A. G. Cullis, W. E. Hagston, and C. R. Whitehouse, J. Cryst. Growth, 150, 176(1995). – for GaAs.
4. R. Smith, Nucl. Instru. Meth. B, 67, 335(1992). – for GaAs.
5. J. Oh, C.H. Grein, J. Crys. Growth, 193, 241 (1998).
6. D. K. Ward, X. W. Zhou, B. M. Wong, F. P. Doty, and J. A. Zimmerman, to be submitted.

Successful Tersoff Potential Growth Simulations

(0001) GaN growth[1] using Tersoff potential[2]

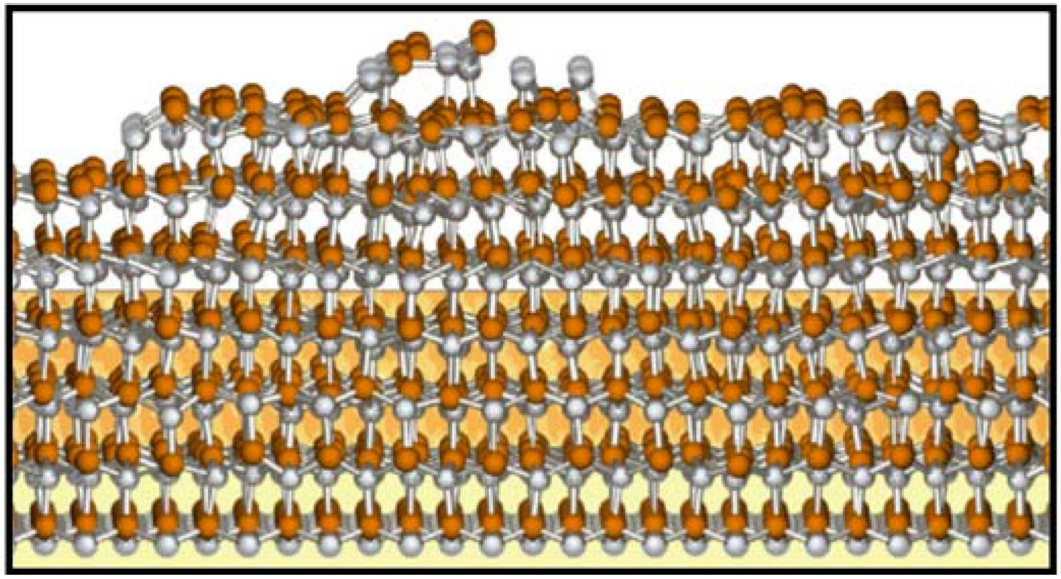

Tersoff-Brenner types of potentials have also been successfully applied for carbon nanotube[3] and SiC[4-6].

1. X. W. Zhou, D. A. Murdick, B. Gillespie, and H. N. G. Wadley, Phys. Rev. B, 73, 45337 (2006).
2. J. Nord, K. Albe, P. Erhart, and K. Nordlund, J. Phys., 15, 5649 (2003).
3. E. H. Feng, and R. E. Jones, Phys. Rev. B, 81, 125436 (2010).
4. H. Yang, X. Hu, and H. Jónsson, Surf. Sci., 316, 181(1994).
5. A. J. Dyson, and P. V. Smith, Surf. Sci., 396, 24 (1998).
6. F. Gao, W. J. Weber, Nuc. Inst. Meth. Phys. Res. B, 191, 504 (2002).

BOP Development …

Bond Order Potential (BOP)

$$E = \frac{1}{2}\sum_i \sum_{j\neq i} \phi_{ij}(r_{ij}) - \sum_i \sum_{j\neq i} \beta_{\sigma,ij}(r_{ij}) \cdot \Theta_{\sigma,ij} - \sum_i \sum_{j\neq i} \beta_{\pi,ij}(r_{ij}) \cdot \Theta_{\pi,ij}$$

$\phi_{ij}(r_{ij})$: core-core repulsion; $\beta_{\sigma,ij}(r_{ij})$ and $\beta_{\pi,ij}(r_{ij})$: σ and π bond integrals describing electron hopping probabilities among different orbital's; $\Theta_{\sigma,ij}$ and $\Theta_{\pi,ij}$: σ and π bond orders describing half of difference in number of electrons in the bonding and anti-bonding states. $\Theta_{\sigma,ij}$ and $\Theta_{\pi,ij}$ are complicated functions of bond length and bond angles.

1. D. G. Pettifor, M. W. Finnis, D. Nguyen-Manh, D. A. Murdick, X. W. Zhou, and H. N. G. Wadley, Mater. Sci. Eng. A, 365, 2 (2004).
2. D. G. Pettifor, and I. I. Oleinik, Phys. Rev. B, 59, 8487 (1999).
3. D. G. Pettifor, and I. I. Oleinik, Phys. Rev. Lett., 84, 4124 (2000).
4. D. G. Pettifor, and I. I. Oleinik, Phys. Rev. B, 65, 172103 (2002).
5. R. Drautz, D. Nguyen-Manh, D. A. Murdick, X. W. Zhou, H. N. G. Wadley, and D. G. Pettifor, TMS Lett., 1, 31 (2004).
6. R. Drautz, D. A. Murdick, D. Nguyen-Manh, X. W. Zhou, H. N. G. Wadley, and D. G. Pettifor, Phys. Rev. B, 72, 144105 (2005).
7. D. A. Murdick, X. W. Zhou, H. N. G. Wadley, D. Nguyen-Manh, R. Drautz, and D. G. Pettifor, Phys. Rev. B, 73, 45206 (2006).

BOP Origin

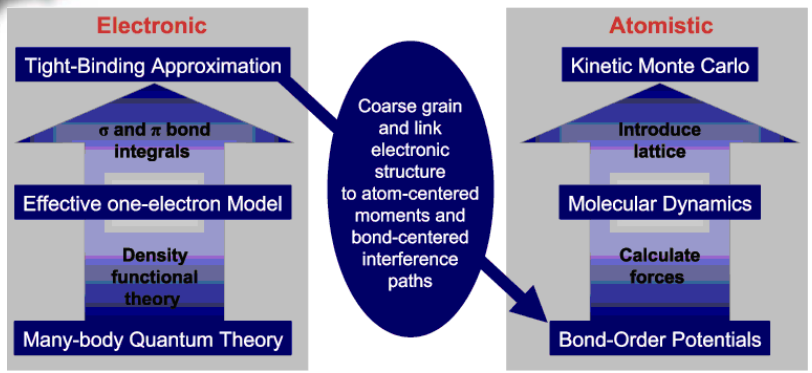

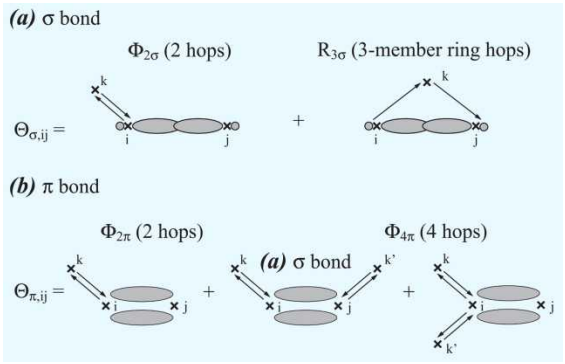

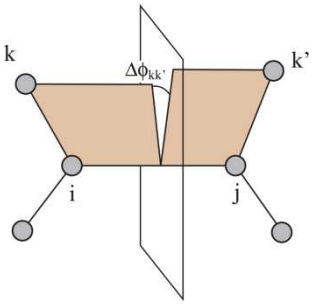

1. **Derived from quantum mechanics theory through systematic coarse-graining;**
2. **Separate treatment of σ and π bonding energies** (products of bond order* and bond integral#);
3. **The first two levels of the expanded Green function retained for the σ and π bond orders;**
4. **Up to four electron hops are considered, naturally incorporating the 3-member ring term in the σ bonding ($R_{3\sigma}$) and the dihedral angle ($\Delta\phi_{kk'}$) effect in the p bonding;**
5. **Valence effect is addressed.**
6. **Accuracy comparable to quantum mechanics and scale comparable to conventional molecular dynamics.**

* bond order: half the difference of electrons in the bond and anti-boding states.
\# bond integral: hopping probability of electrons from one orbital to another.

Sandia National Laboratories

Ideal Atomistic Model for Defects

1. **Transferrable to a variety of configurations: clusters** (dimer, trimer, square, tetrahedron, and chain for elements and compounds; Cd_2Te and $CdTe_2$ trimers for compounds)**, lattices** (diamond-cubic, simple-cubic, body-centered-cubic, face-centered-cubic, hexagonal-close-packed, graphite, graphene, and A8 for elements; zinc-blende, wurtzite, NaCl, CsCl, binary-graphite, AuCu, CuPt, NiAs, CrB, AlSb, binary-graphene, and face-centered-square for the stoichiometric compound CdTe; Ag_2O, CaF_2 for the non-stoichiometric compounds $CdTe_2$ or Cd_2Te)**, and defects** (vacancies, Cd@Te and Te@Cd antisites, Cd and Te interstitials at different locations)**;**
2. **Lowest energy for the equilibrium structure;**
3. **Validatable in vapor- and melt- growth simulations: testing a variety of configurations that are not possible to study directly.**

BOP Goals

Accuracy comparable to quantum mechanics and scale comparable to conventional molecular dynamics

- **Bond order potential (BOP) is derived from quantum mechanics theories;**
- **We will develop a CdTe BOP and validate it against clusters** (dimer, trimer, square, tetrahedron, and chain for elements and compounds; Cd_2Te and $CdTe_2$ trimers for compounds)**, lattices** (diamond-cubic, simple-cubic, body-centered-cubic, face-centered-cubic, hexagonal-close-packed, graphite, graphene, and A8 for elements; zinc-blende, wurtzite, NaCl, CsCl, binary-graphite, AuCu, CuPt, NiAs, CrB, AlSb, binary-graphene, and face-centered-square for the stoichiometric compound CdTe; Ag_2O, CaF_2 for the non-stoichiometric compounds $CdTe_2$ or Cd_2Te)**, and defects** (vacancies, Cd@Te and Te@Cd antisites, Cd and Te interstitials at different locations)**;**
- **We will also validate the BOP using melt- and vapor- phase growth simulations.**

{Two-step Parameterization + Vapor Deposition Validation }: Thousand Iterations

1. **For the nearest neighbor structures** (e.g., dimer, dc, sc, fcc, hcp, NaCl, zb, etc.), $E_b = \phi(r) - 2\beta_\sigma(r) \cdot\Theta_\sigma - 2\beta_\pi(r) \cdot\Theta_\pi = \phi(r) - 2\beta_\sigma(r) \cdot(c_1\cdot\Theta_\sigma + c_2 \cdot\Theta_\pi)$, **where c_1, are c_2 constants;**
2. **Under hydrostatic strain, the bond orders Θ_σ and Θ_π are constant. From the equilibrium condition $\partial E_b/\partial r = 0$, $c_1\cdot\Theta_\sigma + c_2 \cdot\Theta_\pi = \phi'(r)/2\beta_\sigma'(r)$;**
3. **The equilibrium bond energy $E_{b,0}$ and its second derivative $E''_{b,0}$ as a function of the equilibrium bond length r_0 can be expressed as $E_{b,0} = \phi(r) - \beta_\sigma(r) \cdot\phi'(r)/\beta_\sigma'(r)$ and $E''_{b,0} = \phi''(r_0) - \beta_\sigma''(r) \cdot\phi'(r)/\beta_\sigma'(r)$ respectively;**
4. **The first step is to optimize the parameters in the pair functions $\phi(r)$ and $\beta_\sigma(r)$ using the target lattice constants, cohesive energies, and bulk moduli of a variety of the nearest neighbor structures;**
5. **The second step is then to fit bond order parameters by fitting to the bond order of the nearest neighbor structures and various properties of the non-nearest neighbor structures.**

1. K. Albe, K. Nordlund, J. Nord, and A. Kuronen, Phys. Rev. B, 66, 35205 (2002).
2. J. Nord, K. Albe, P. Erhart, and K. Nordlund, J. Phys., 15, 5649 (2003).

BOP Captures Many Cd, Te, and CdTe Phases

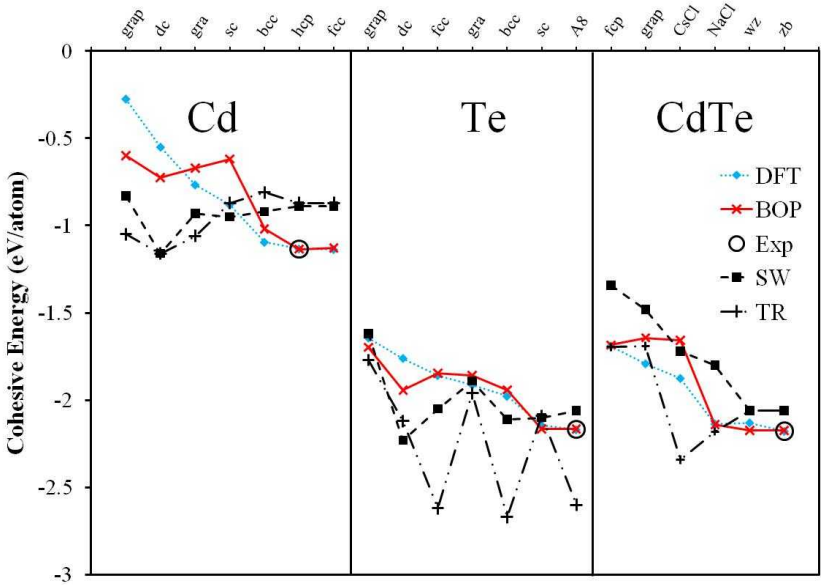

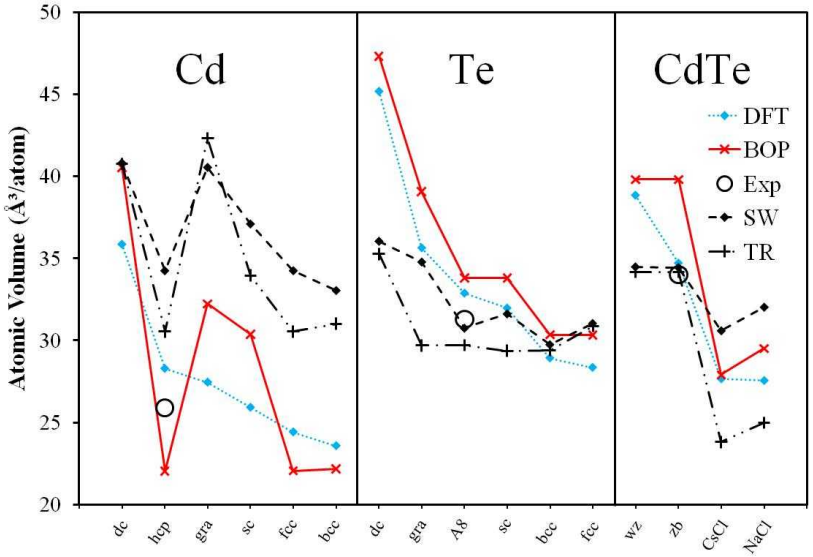

Have validated against clusters (dimer, trimer, square, tetrahedron, and chain for elements and compounds; Cd_2Te and $CdTe_2$ trimers for compounds)**, lattices** (diamond-cubic, simple-cubic, body-centered-cubic, face-centered-cubic, hexagonal-close-packed, graphite, planer-graphite, and A8 for elements; zinc-blende, wurtzite, NaCl, CsCl, binary-graphite, AuCu, CuPt, NiAs, CrB, AlSb, planar-binary-graphite, and face-centered-square for the stoichiometric compound CdTe; Ag_2O, CaF_2 for the non-stoichiometric compounds $CdTe_2$ or Cd_2Te)**, and defects** (vacancies, Cd@Te and Te@Cd antisites, Cd and Te interstitials at different locations)

Other Properties

Elastic Constants of zinc-blende CdTe (GPa)

C_{ij}	experiment (300K)[1]	DFT[2]	BOP	Tersoff-Rockett[3]	Stillinger-Weber[4]
C_{11}	53.3	53.2	49.5	50.7	44.3
C_{12}	36.5	36.0	31.3	37.5	19.6
C_{44} (relaxed)	20.4	---	---	15.2	18.0
C_{44} (unrelaxed)	---	31.8	40.6	46.8	30.7

Defect energies of zinc-blende CdTe (eV)

defect type	DFT	BOP	Tersoff-Rockett[3]	Stillinger-Weber[4]
Cd vacancy	2.20	2.66	2.43	2.60
Te vacancy	2.72	1.64	0.93	1.53
Cd antisite	3.01	3.24	0.18	0.80
Te antisite	3.16	2.04	1.19	0.74
Cd in Cd interstitial	1.98	1.21	1.36	4.27
Te in Cd interstitial	3.52	2.92	0.55	2.60
Cd in Te interstitial	2.14	2.12	0.61	3.76
Te in Te interstitial	3.91	2.92	1.28	3.57

1. J. M. Rhowe, R. M. Nicklow, D. L. Price, and K. Zanio, Phys. Rev. B, 10, 671 (1974).
2. B. K. Agrawal, and S. Agrawal, Phys Rev. B, 45, 8321(1992).
3. J. Oh, and C. H. Grein, J. Crys. Growth, 193, 241 (1998).
4. Z. Q. Wang, D. Stroud, and A. J. Markworth, Phys. Rev. B, 40, 3129 (1989).

Cd and Te Vapor Growth Simulations

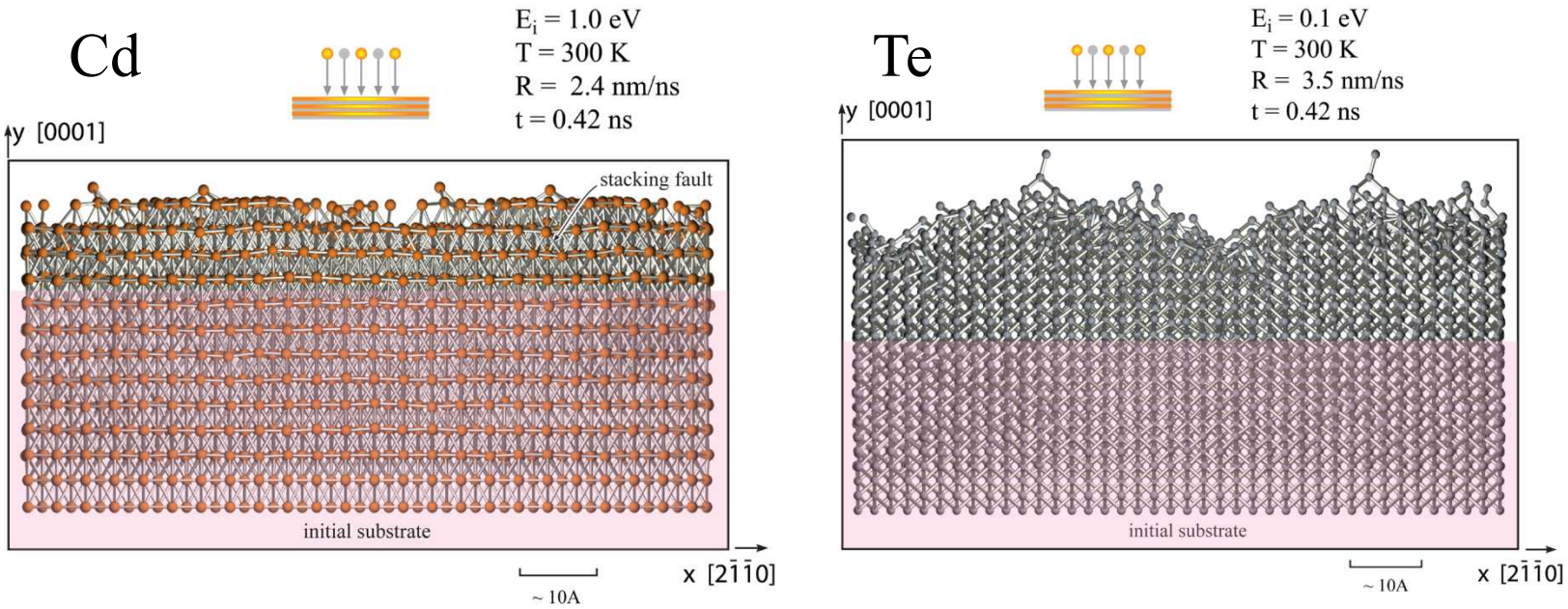

Crystalline growth was obtained for Cd and Te elemental growth as well as CdTe compound growth.

An Example Vapor Deposition Simulation

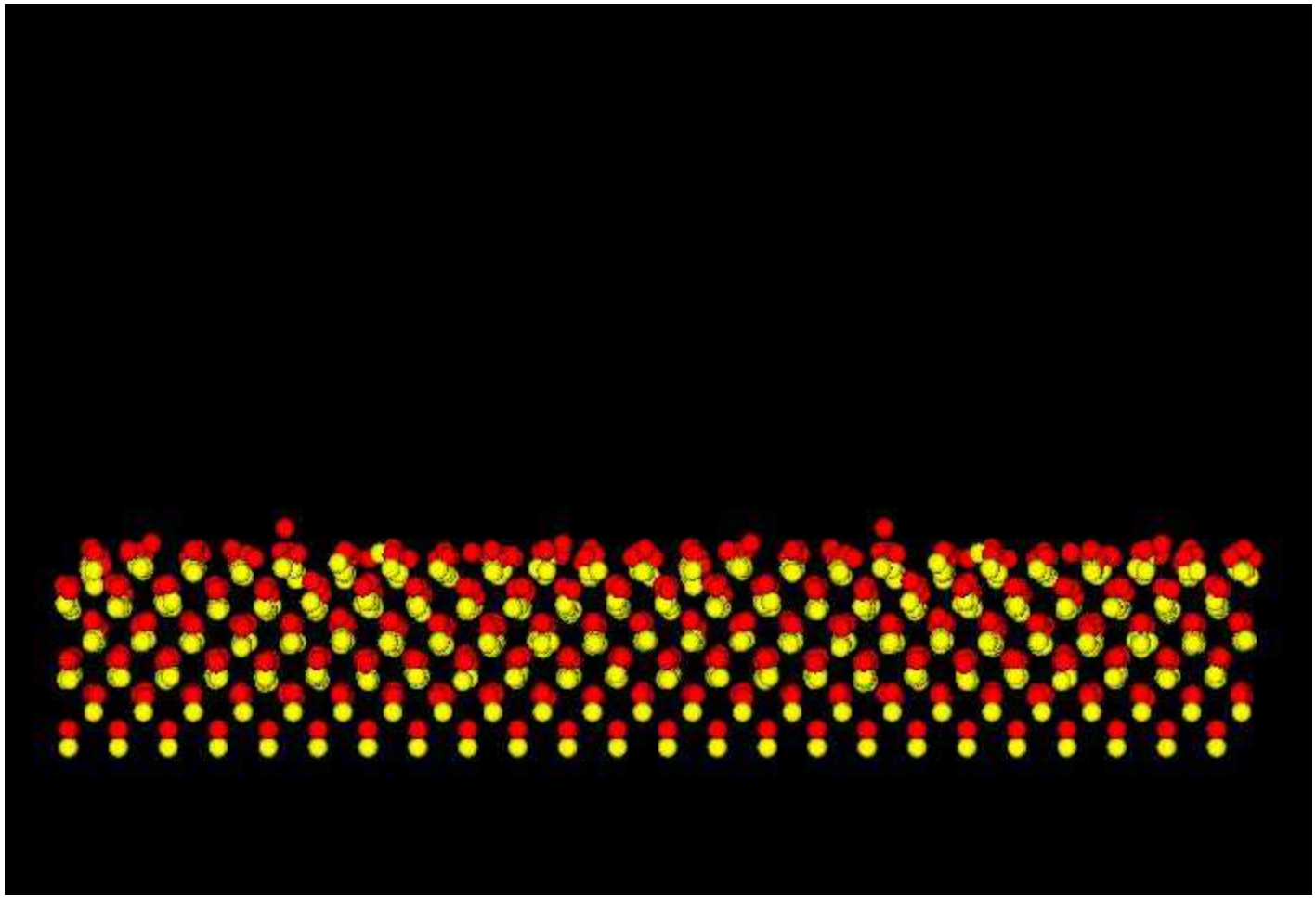

Substrate temperature 1200K; adatom energy 0.1 eV; vapor species Cd + Te_2; deposition rate 2.7 nm/ns

CdTe Vapor Growth Simulations

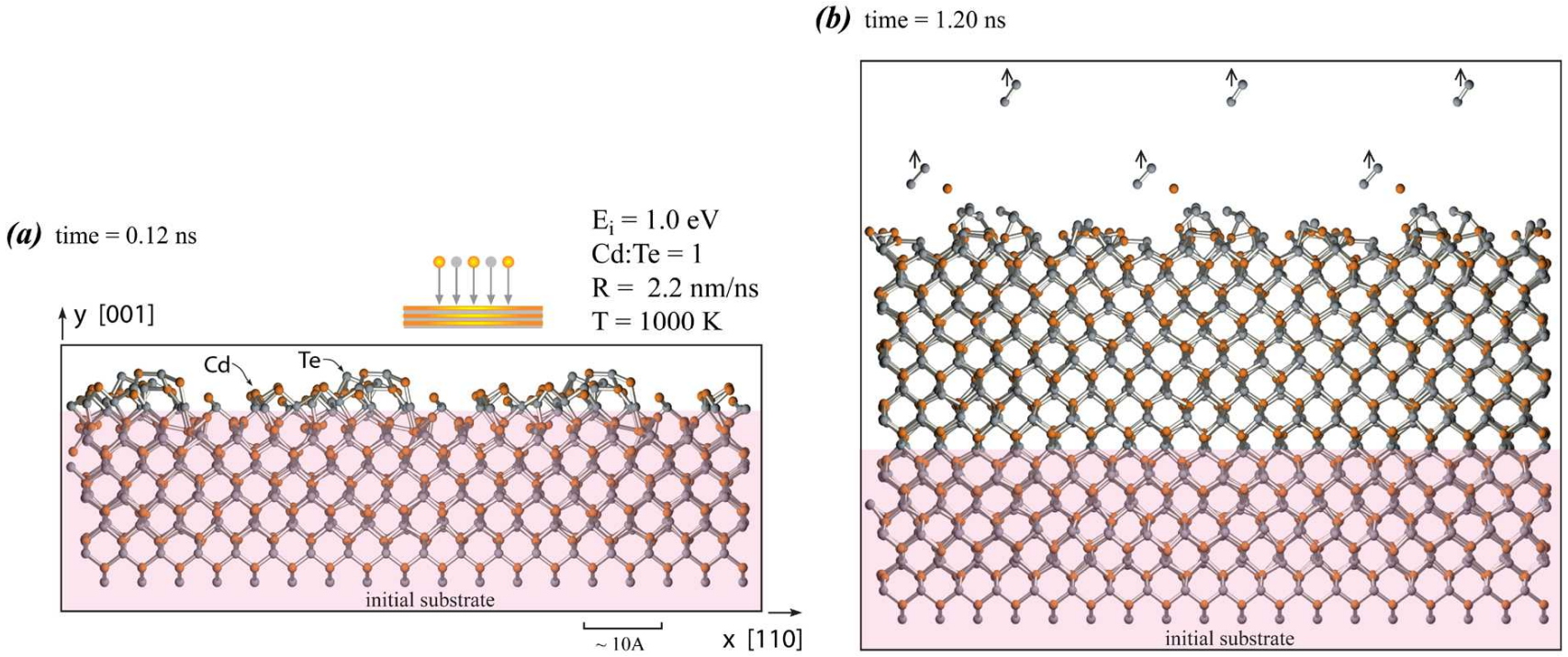

Our recent work on CdTe. Te was seen to evaporate as Te_2, and such a phenomenon cannot be captured by SW potential.

MD Simulations of Misfit Dislocation Formation

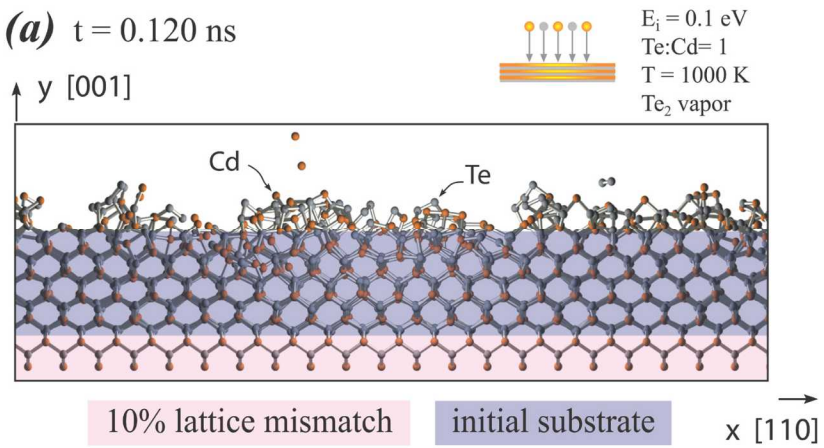

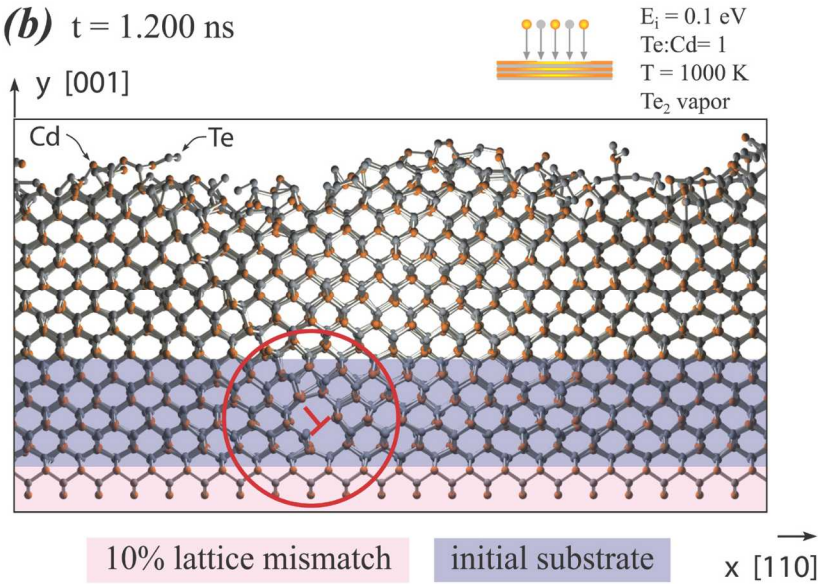

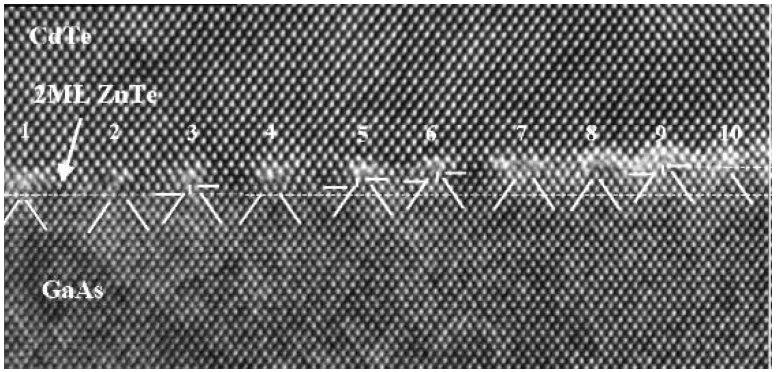

Similar misfit dislocation structures observed from HRTEM experiment in GaAs/ZnTe/CdTe samples. S. Kret, P. Dluzewski, P. Dluzewski, and J.-Y. Laval, Phil. Mag., 83, 231 (2003).

MD Simulation of Melt-Growth of CdTe

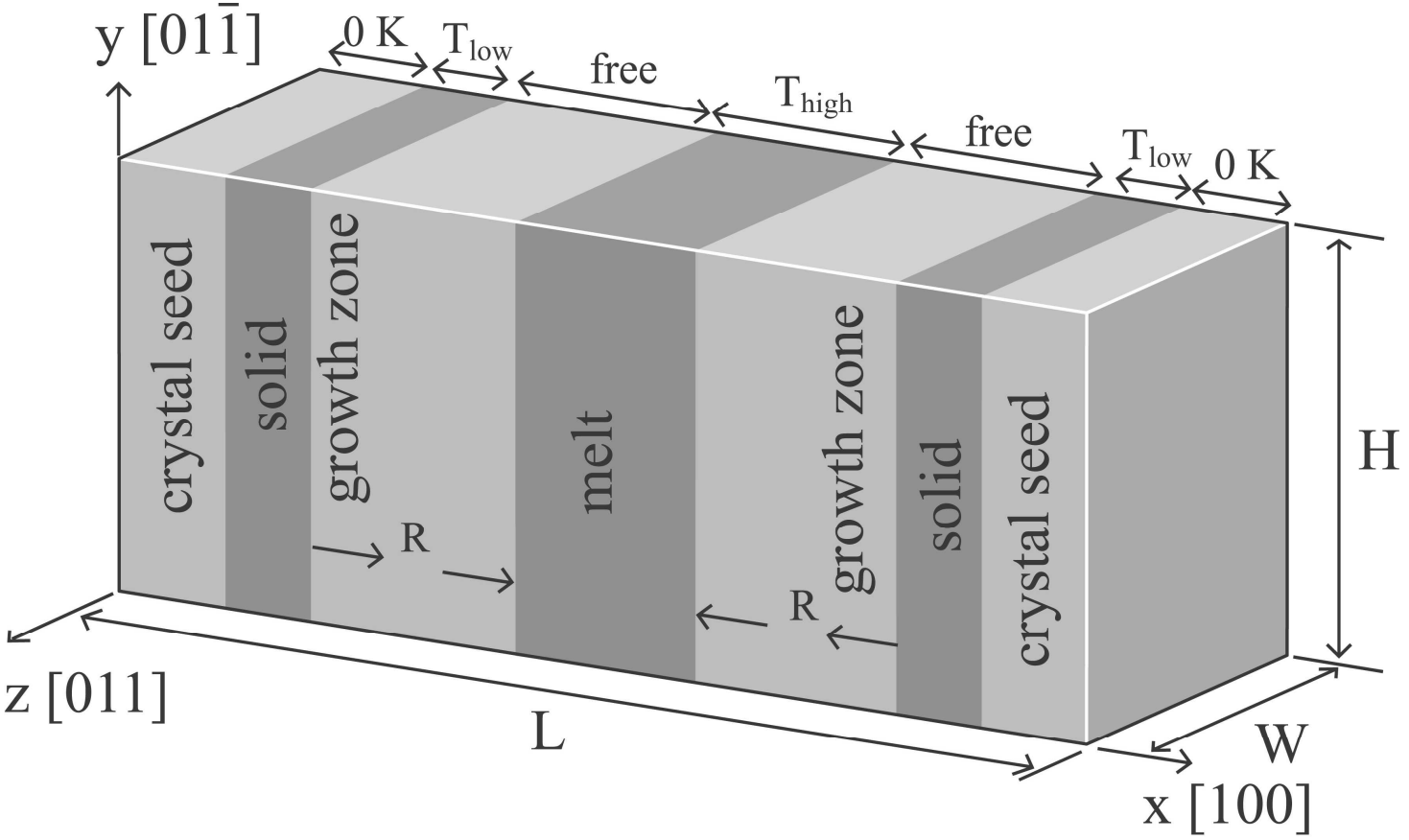

Sandia National Laboratories

An Example at T_{low}=1000K, T_{high}=2200K, R = 0.2 Å/ps

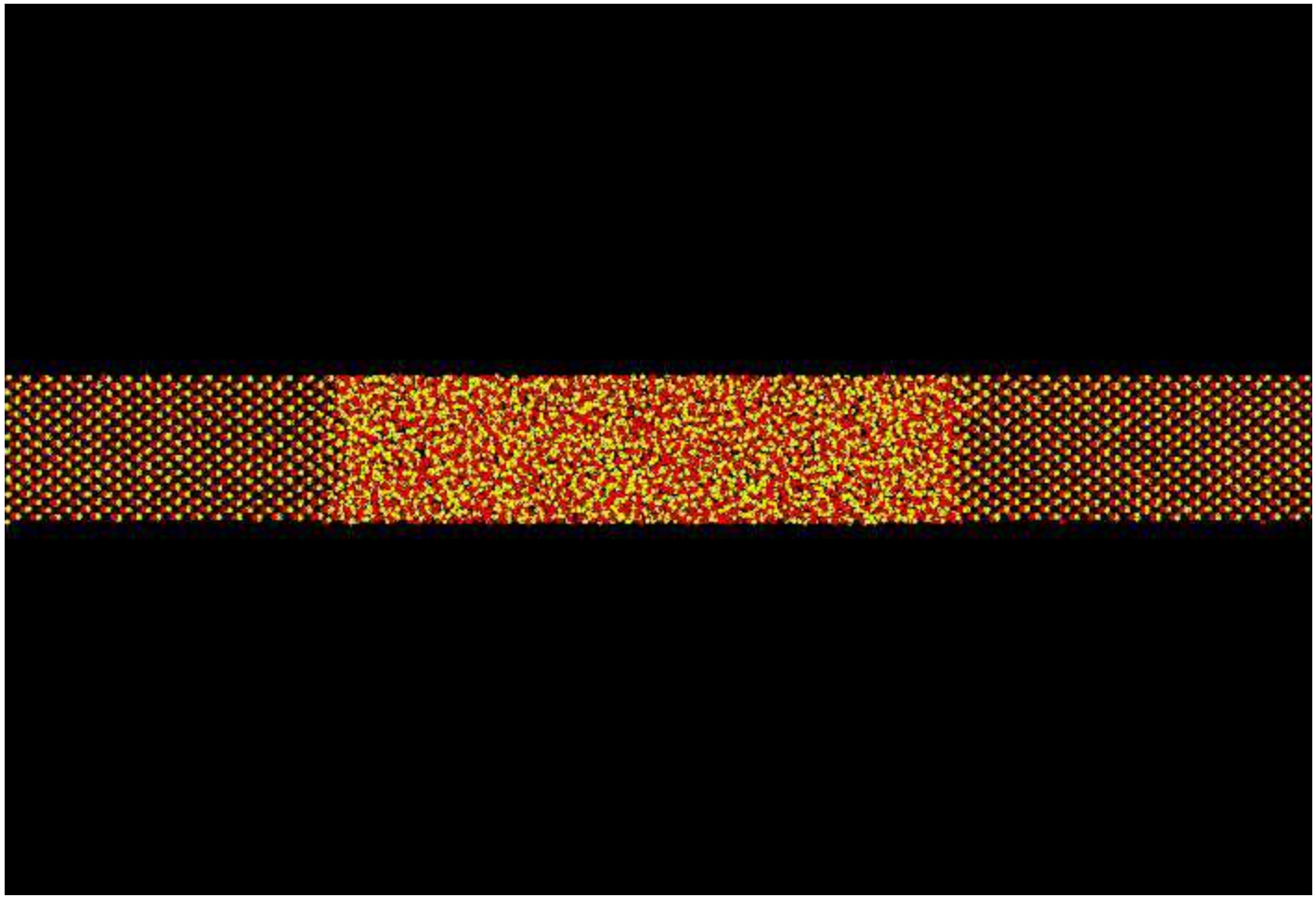

Growth Observation

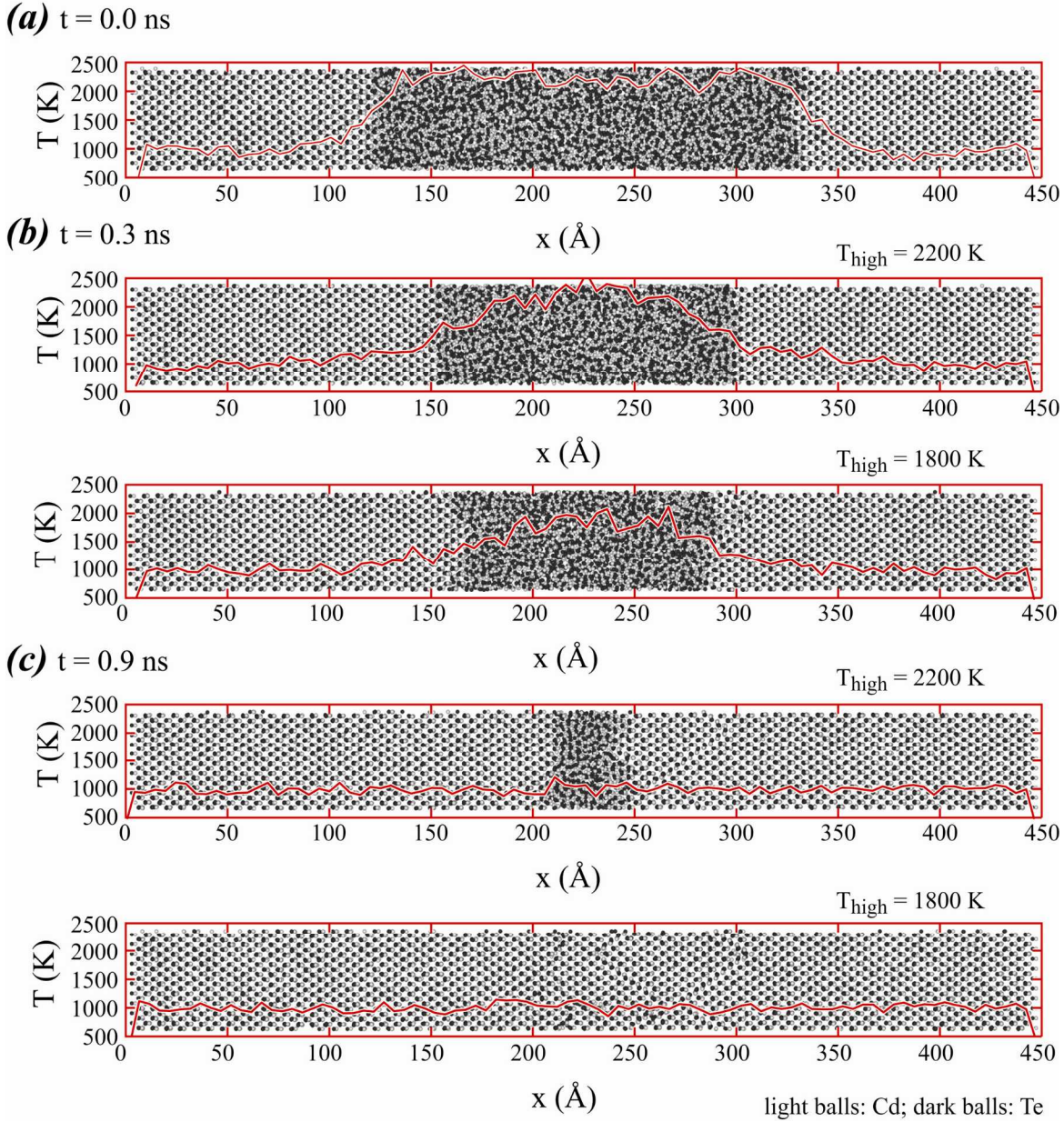

Quality of the Grown Crystals

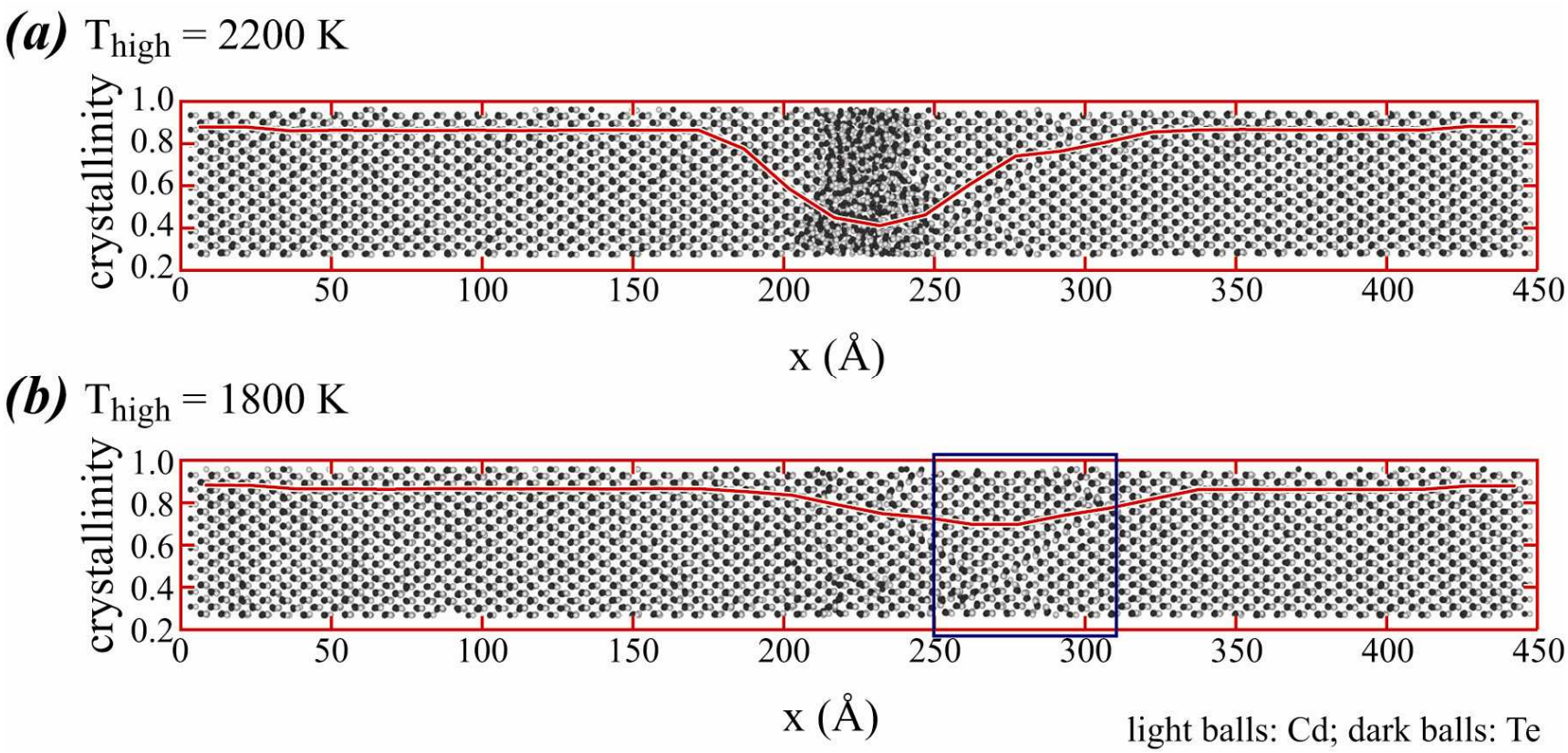

Discovery of Stacking Fault Defects

(a) framed region in Fig. 4(b)

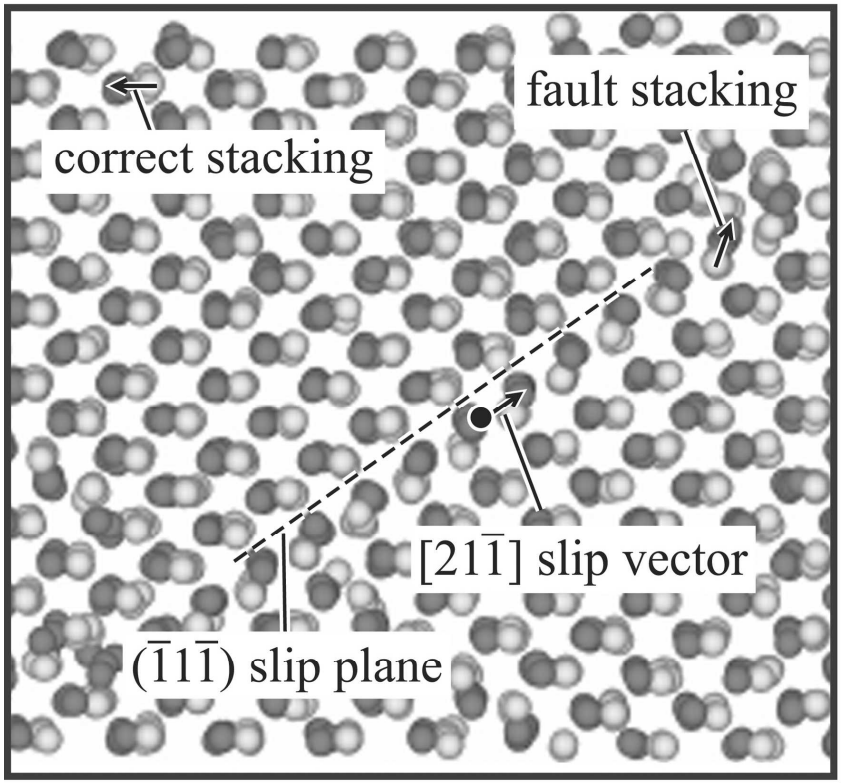

(b) defect nucleation at local facets

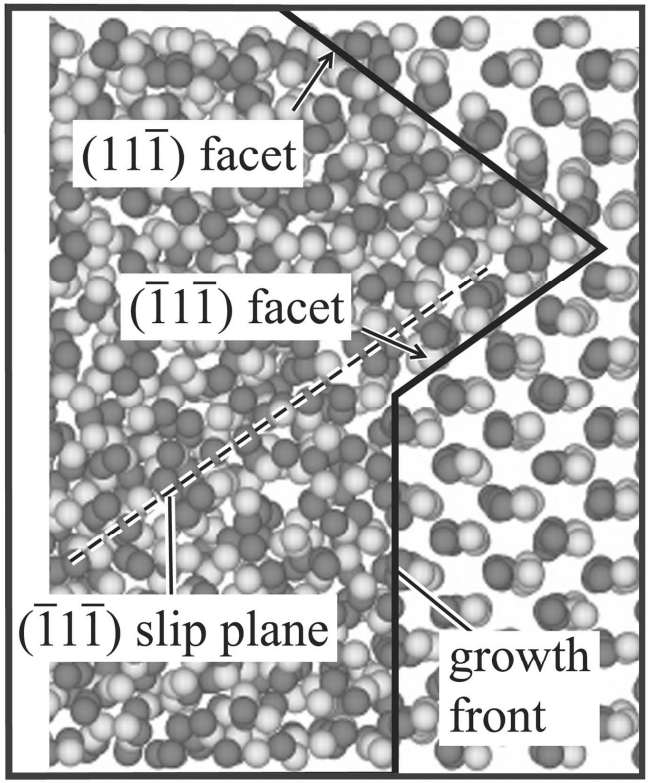

Dislocation Models

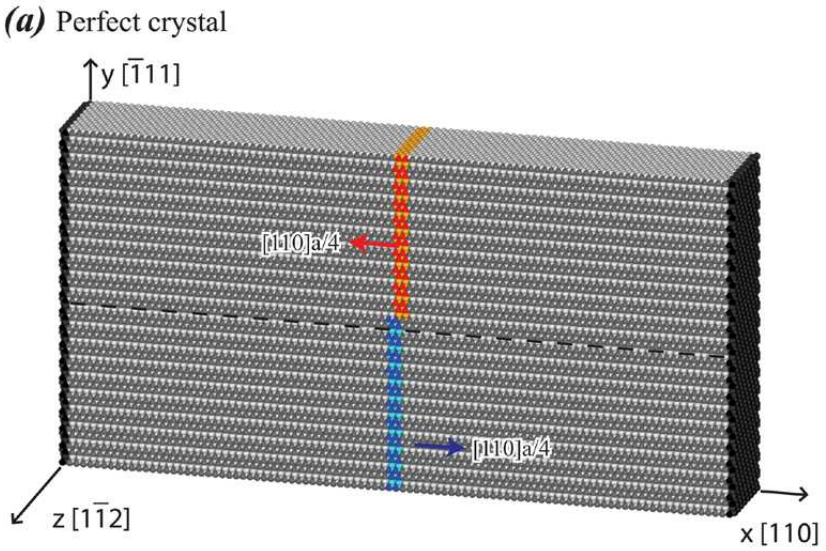

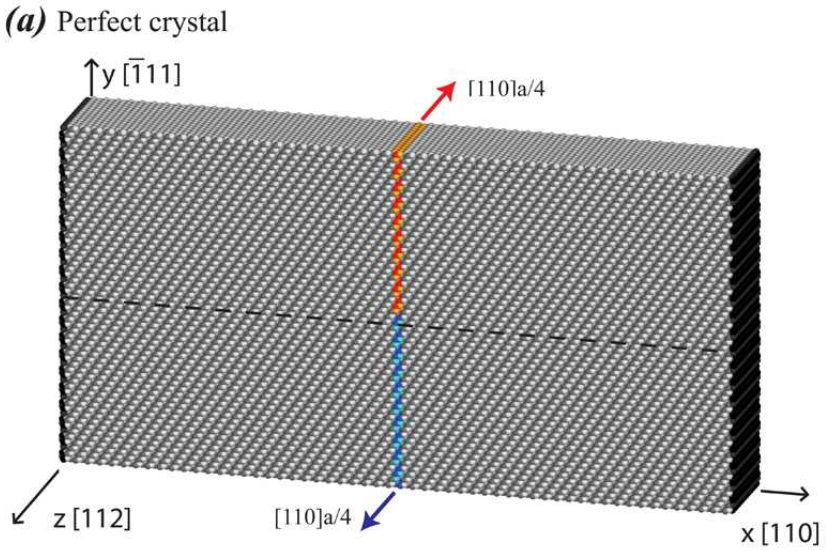

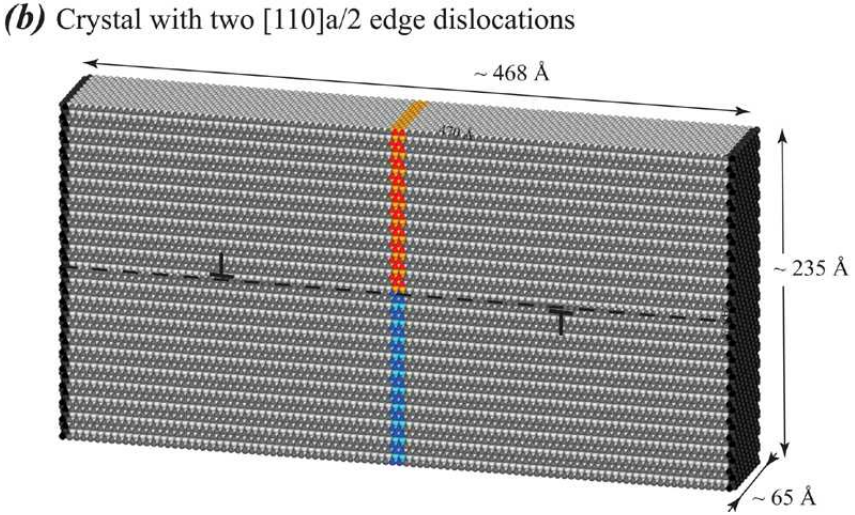

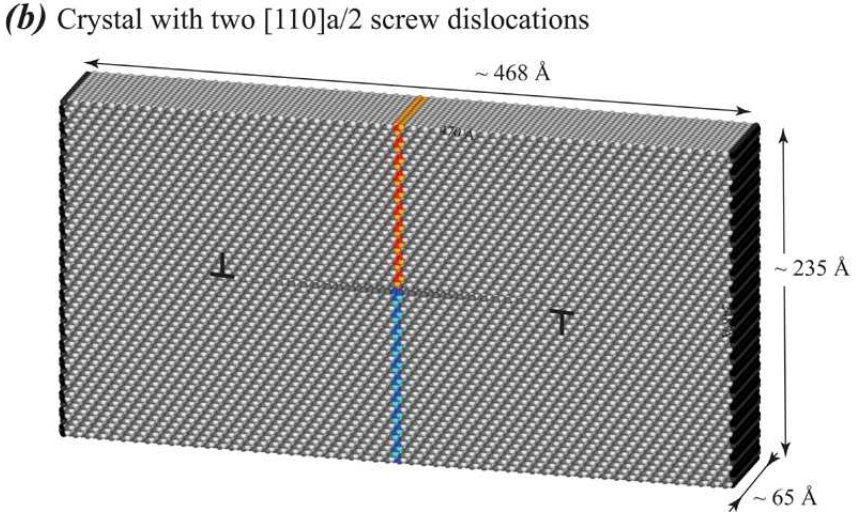

Dislocation Energies/Configurations in CdTe

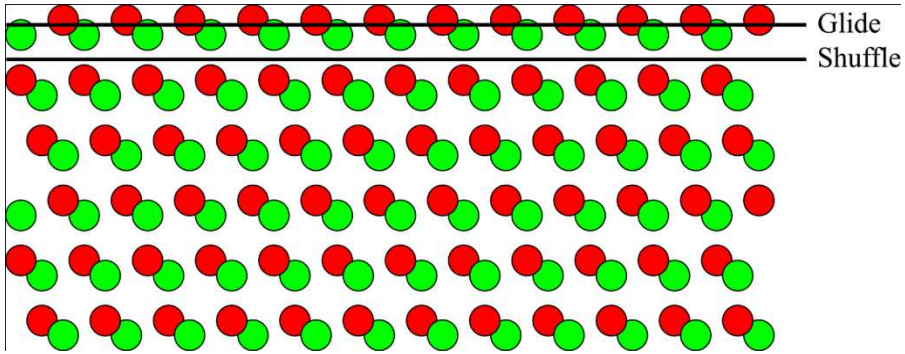

Dislocation line energies (eV/Å)

edge		screw	
shuffle	glide	shuffle	glide
1.66	> 4.0	0.83	> 3.8

Edge shuffle dislocation configurations (top view of two planes)

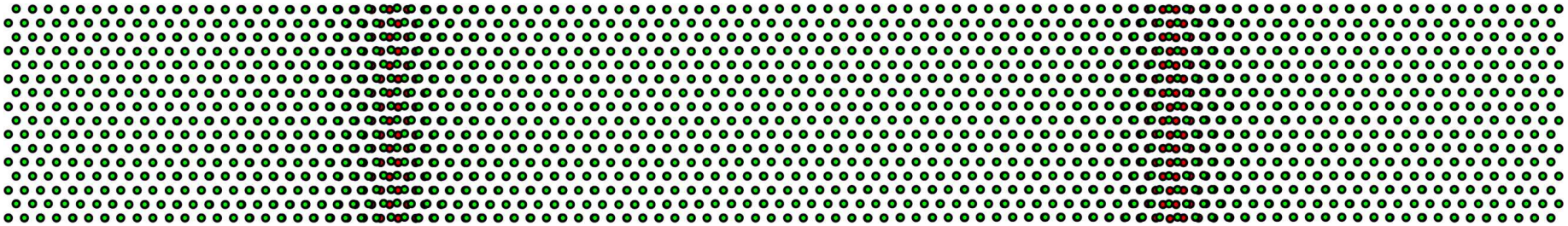

Screw shuffle dislocation configurations (top view of two planes)

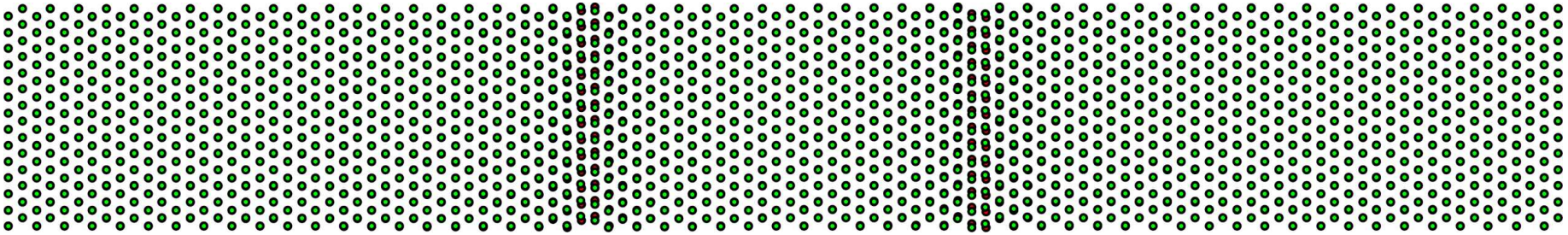

Sandia National Laboratories

Dislocation Loop Configurations in CdTe

Loop creation

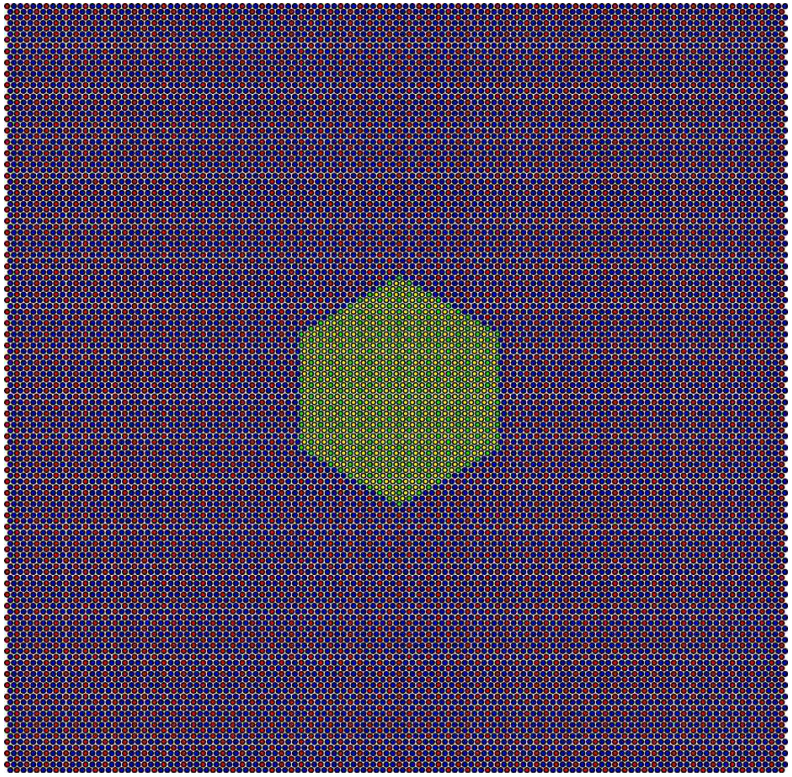

After relaxation

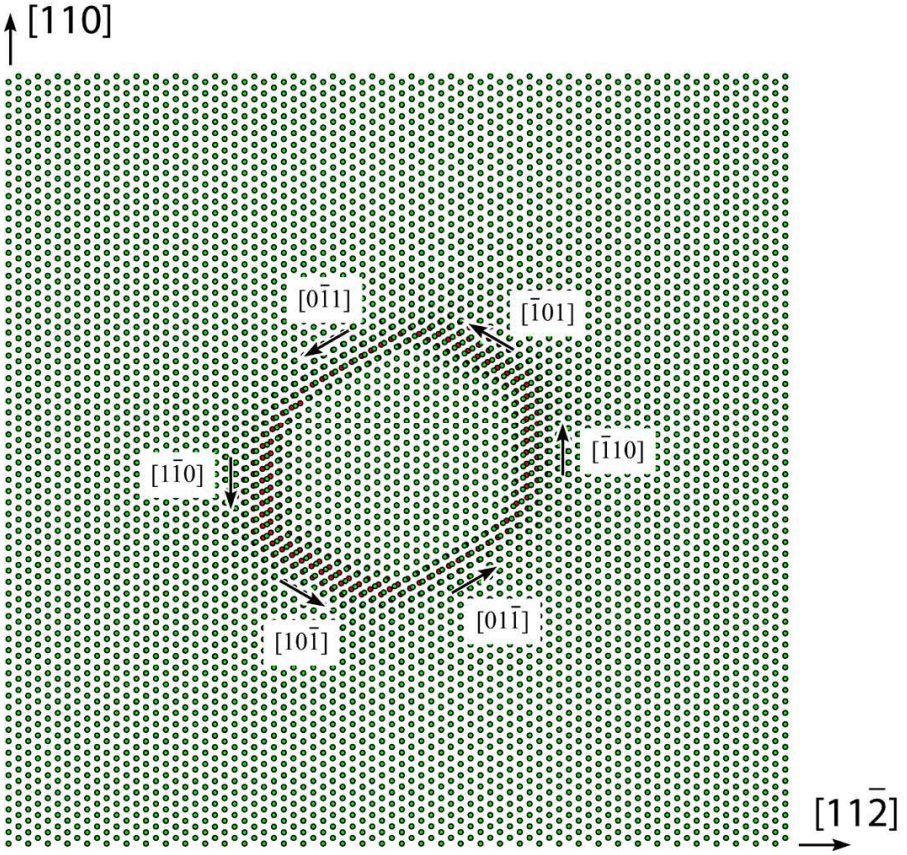

1. Graded spreading instead of partial dislocations;
2. 60^{o} dislocations;
3. Dislocations: nucleation sites for precipitates;
4. Displacement filed results in electric field.

Zn Vapor Growth Simulations

Zn

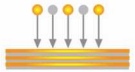

E_i = 0.1 eV
T = 400 K
R = 1.9 nm/ns
t = 0.42 ns

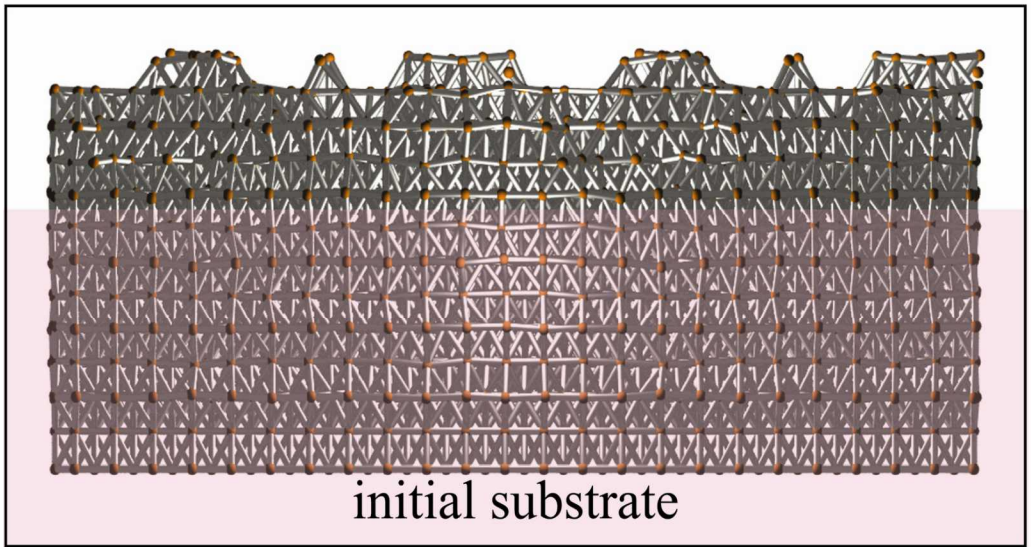

Crystalline growth was obtained for Zn.

Future Work for the Remainder of the Project

- **Theoretical Work**
  - Perform quantum-mechanical calculations on lattice constants, cohesive energies, elastic constants, defect energies, and surfaces reconstructions of a variety Zn, ZnTe, CdZn, and CdZnTe phases.
  - Develop BOPs for Zn, ZnTe, CdTe, and CdZnTe systems.
  - Improve algorithm of BOPs calculations in LAMMPS.
  - Perform large scale simulation on various possible dislocation configurations, characteristics, stress field, and interaction with other defects (in particular on precipitate formation).
  - Perform large scale simulations on small scale defect evolution under thermomechanical conditions
- **Experiments**
  - In conjunction with crystal growth work at PNNL, perform SEM CL analysis of dislocations in as-grown CZT samples.
  - Use the input from theoretical work to design improved growth of CZT crystals.

Acknowledgement

This work is supported by the NNSA/DOE Office of Nonproliferation Research and Development, Proliferation Detection Program, Advanced Materials Portfolio. Sandia National Laboratories is a multi-program laboratory managed and operated by Sandia Corporation, a wholly owned subsidiary of Lockheed Martin Corporation, for the U.S. Department of Energy's National Nuclear Security Administration under contract DE-AC04-94AL85000.